Supplementary Text and Figures

Nanobody-aided structure determination of the EpsI:EpsJ pseudopilin heterodimer from *Vibrio vulnificus*

Anita Y. Lam[1,2], Els Pardon[3,4], Konstantin V. Korotkov[1], Wim G. J. Hol[1,2*] and Jan Steyaert[3,4*],

[1]Department of Biochemistry, [2]Biomolecular Structure & Design Program, Biomolecular Structure Center, University of Washington, Seattle, WA 98195, USA;

[3]Department of Molecular and Cellular Interactions, VIB, B-1050 Brussels, Belgium

[4]Structural Biology Brussels, Vrije Universiteit Brussel, B-1050 Brussels, Belgium

*Corresponding authors' email addresses:

wghol@u.washington.edu, jan.steyaert@vub.ac.be

Supplementary Text

EpsI:EpsJ in two different crystal structures and SER mutations

The EpsI:EpsJ heterodimer in our EpsI:EpsJ:Nb11 ternary complex is similar to the EpsI:EpsJ heterodimer itself, as reflected in an RMSD of 1.1 Å for 222 equivalent C^{α} atoms. It is interesting to look into the role of the residues Glu96 and Lys97 of EpsI in the two crystal forms used for solving the EpsI:EpsJ structure of Yanez et al. (2008) and the current structure. The SER mutations of these two residues in the previous structure (Yanez et al., 2008), which altered both side chains to a Thr, allowed for formation of the triclinic crystals used for that study. An abundance of steric clashes of less than 2 Å would have occurred if the threonine residues were to remain Glu96 and Lys97, thereby rendering that particular triclinic crystal form unlikely to grow from the wild-type protein (Yanez et al., 2008). In the ternary complex crystals in the present structure, Glu96 and Lys97 of EpsI are preserved and make crystal contacts with symmetry mates in two of the four copies of EpsI per asymmetric unit. The $O^{\varepsilon 2}$ of Glu96 in EpsI makes contacts with N of Ile28 of EpsI' while the N^{ζ} of Lys97 interacts with $O^{\delta 2}$ of Asp154 of EpsI'. Clearly, the SER mutations of EpsI were essential to obtain suitable EpsI:EpsJ crystals by Yanez et al. (2008) whereas the wild type side chains most likely promoted crystal growth for the present EpsI:EpsJ:Nb11 structure.

EpsJ:Nb11 interactions

Of the 26 interface residues in EpsJ, ten residues are engaged in making twelve inter-protein hydrogen bonds and fifteen residues make van der Waals contacts with Nb11. The residues making H-bonds can be subdivided into CDR1-interacting (Asp 83-$O^{\delta 2}$, Lys116-N^{ζ}, Asp117-$O^{\delta 2}$, Arg119-$N^{\eta 2}$) and CDR3-interacting (Asn66-O&$O^{\delta 1}$, Arg114-$N^{\eta 2}$, Trp125-$N^{\varepsilon 1}$, Gln134-N^{H}&O, Gly136-NH). Finally, EpsJ contributes one van der Waals contact (Glu121) with CDR1, three with CDR2 (Glu68, Try80, Ser84), and eleven with CDR3 (Thr65, Gly67, Leu82, Lys110, Val123, Asp129, Thr130, Pro131, Gly133, Glu135, Val138).

An extensive loop of Nb11 buries itself into a pocket of EpsJ. The negative charge of $O^{\delta 1}$ and $O^{\delta 2}$ of Asp129 and the main-chain oxygen of Arg64 inside the EpsJ pocket and of $O^{\gamma 1}$ of Thr65 on the rim of the pocket interact favorably with the positive charge of Arg102 and the main-chain N of Gly101 on the CDR3 bulge ("PDB entry 3CFI residue numbering" is used; see upper line Figure 1A of the main text. The corresponding "IMGT numbering" is shown in the lower line of Figure 1A. of the main text). The positive charges of Lys110 plus $N^{\varepsilon 1}$ Trp125 and $N^{\varepsilon 2}$ of Gln134 in the EpsJ pocket

are complementary to the main-chain O of both Leu99 and Gly100, and the $O^{\delta 1}$ and $O^{\delta 2}$ of Asp103 on the nanobody.

Additionally, the contacts of residues surrounding the CDR3-binding EpsJ pocket are likely to contribute to the tight binding of Nb11, including the main-chain O and $O^{\delta 1}$ of Asn66; the main-chain O of Pro131; and the main-chain O of Ala132 of EpsJ. These atoms outside the EpsJ pocket interact with the guanidinium group of Arg102 and the main-chain NH of the conserved framework residue, Trp47, of the nanobody.

Supplementary Figures

Supplementary Figure S1: IMGT "Collier de Perles" representation of Nb11.

The graphical representation of the nanobody sequence shows the CDR1 (red), CDR2 (orange), and the CDR3 (purple). Hydrophobic residues are highlighted with light blue fill, prolines with pale yellow fill. The β-strand order and directionality are shown on the bottom. In this Figure S1, the residues are numbered with standard IMGT numbering (Lefranc, 2005) are used. In contrast, throughout elsewhere manuscript the contiguous "PDB numbering" of our deposited entry with PDB code 3CFI is used to have a direct connection with the deposited coordinates and sequence. For correlating the two sequence numbering systems see the upper and lower lines in Figure 1A of the main text.

Several nanobodies have (Desmyter et al., 1996; Decanniere et al., 1999; Desmyter et al., 2001) a second disulfide bridge between CDR1 and CDR3 in addition to the canonical disulfide bridge, formed in Nb11 between Cys22 (PDB numbering, which corresponds to Cys23 IMGT) and Cys95 (PDB)/ Cys104 IMGT). However, Nb11 contains only the canonical disulfide bridge bridge. Interestingly, none of the other nanobodies against EpsI:EpsJ have any other cysteines than the two canonical ones that are also in Nb11 (Figure 1A in the main text).

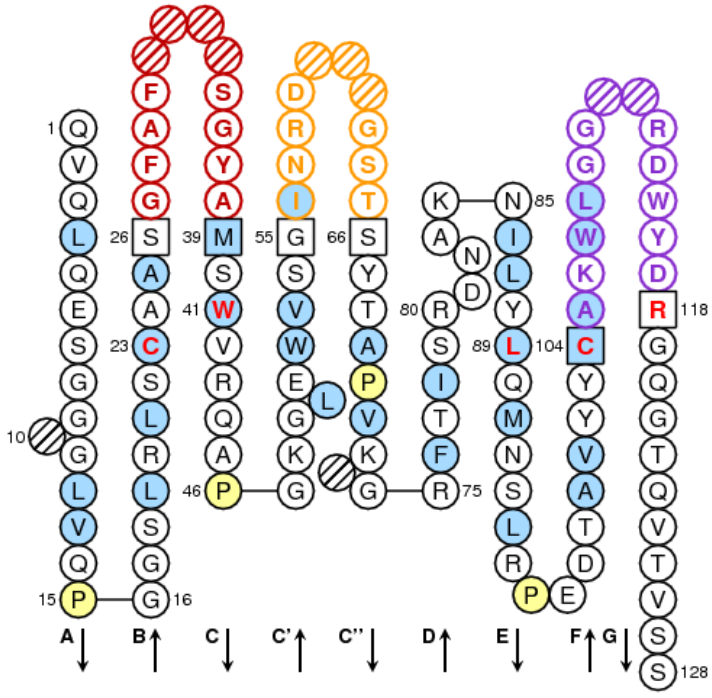

Supplementary Figure S2: Comparison of Nb11 with nearest DALI matches

S2A. Alignment of Nb11 (top line) with the best overall DALI match (1IGT; Z=20.4; middle line) and best nanobody DALI match (1ZVH; lower line) (De Genst et al., 2006) with a Z-score of 17.5. The CDR regions are boxed. CDR1, green; CDR2, purple; CDR3, red. (Note: For Nb11, contiguous "PDB entry 3CFI residue numbering" is used; the same as in the upper line of Figure 1A in the main text. The corresponding "IMGT numbering" is shown in the lower line of Figure 1A in the main text.)

S2B. Structural superposition of Nb11 with 1IGT, the VH of a mouse antibody (Holm and Sander, 1993). Nb11, orange; 1IGT, cyan; CDR1, green shades; CDR2, purple shades; CDR3, red shades. The darker colored CDRs represent those from Nb11, while the lighter colored CDRs belong to 1IGT. With a Z-score of 20.4, and an RMSD of 1.0 Å for 109 structurally equivalent C^{α} atoms, this stereo figure shows that the two structures are for the most part the same, with large differences in the CDR regions, especially CDR3, as expected.

S2C. Structural superposition of Nb11 with 1ZVH, the nanobody from a hen egg white lysozyme:nanobody complex (De Genst et al., 2006). Nb11, orange; 1ZVH, cyan; CDR1, green shades; CDR2, purple shades; CDR3, red shades. The darker colored CDRs represent those from Nb11, while the lighter colored CDRs belong to 1ZVH. The Z-score is 17.5 and the RMSD is 1.2 Å for 111 structurally equivalent C^{α} atoms. This stereo figure shows that the CDR regions in 1ZVH are much more different from Nb11 than 1IGT, with major differences in both the CDR1 and CDR3 regions. CDR3 of 1ZVH is seven residues longer than Nb11 or 1IGT (Supplementary Figure S2A).

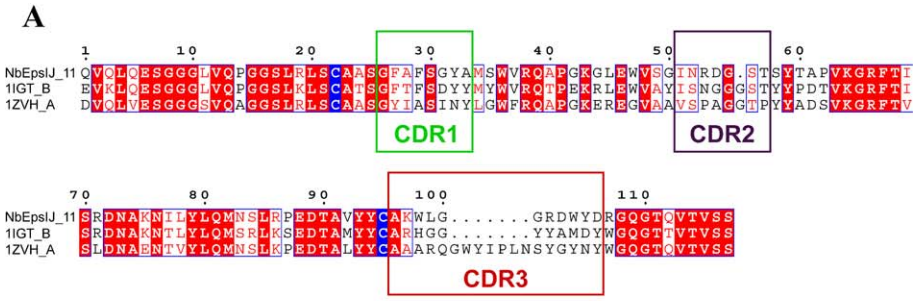
A
NbEpsIJ_11
1IGT_B
1ZVH_A
CDR1
CDR2
CDR3

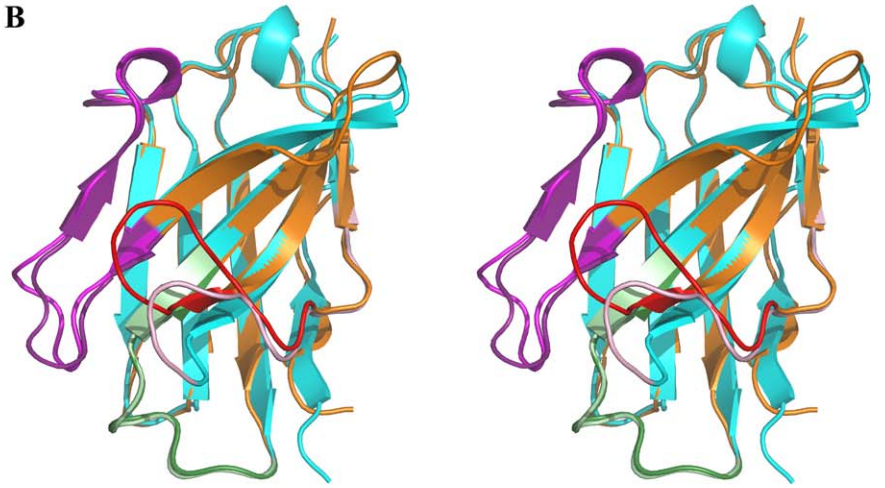
B

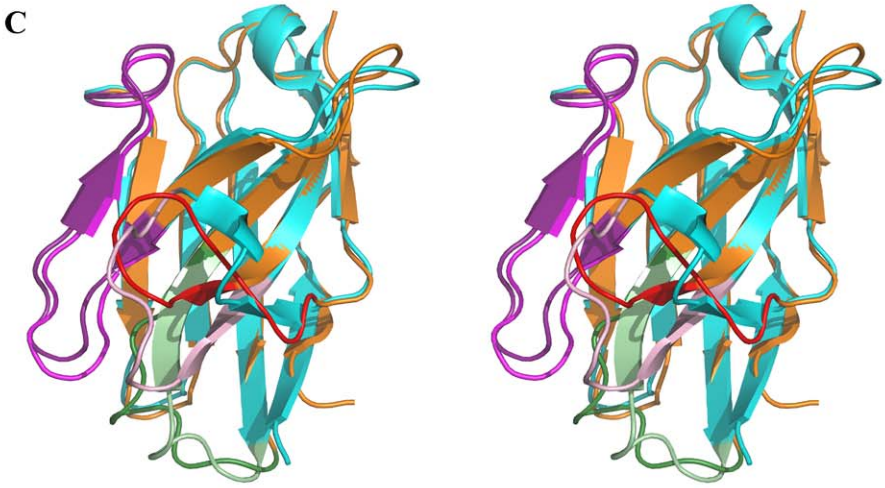
C

Supplementary Table 1: Interactions between Nb11 and EpsJ

Nb11 residue[a]	**Residue Category**	**Type of interaction with EpsJ**
Phe27	CDR1	van der Waals
Ala28	CDR1	van der Waals
Gly31	CDR1	Hydrogen bond
Tyr32	CDR1	Hydrogen bond
Ala33	CDR1	Hydrogen bond
Trp47	Framework	Hydrogen bond
Asn52	CDR2	van der Waals
Arg53	CDR2	$N^{\eta 1}$ Salt bridge with $O^{\delta 1}$ of Asp85 of EpsJ
Thr57	CDR2	van der Waals
Ser58	CDR2	van der Waals
Thr60	CDR2	van der Waals
Trp98	CDR3	van der Waals
Leu99	CDR3	van der Waals
Gly100	CDR3	van der Waals
Gly101	CDR3	van der Waals
Asp106	CDR3	van der Waals
Arg107	CDR3	van der Waals

[a] For Nb11, contiguous "PDB entry 3CFI residue numbering" is used; see upper line Figure 1A in the main text, and of Supplementary Figure S2A. The corresponding "IMGT numbering" is shown in the lower line of Figure 1A in the main text.

Supplementary References

De Genst, E., Silence, K., Decanniere, K., Conrath, K., Loris, R., Kinne, J., Muyldermans, S., and Wyns, L. (2006). Molecular basis for the preferential cleft recognition by dromedary heavy-chain antibodies. Proc Natl Acad Sci U S A *103*, 4586-4591.

Decanniere, K., Desmyter, A., Lauwereys, M., Ghahroudi, M.A., Muyldermans, S., and Wyns, L. (1999). A single-domain antibody fragment in complex with RNase A: non-canonical loop structures and nanomolar affinity using two CDR loops. Structure *7*, 361-370.

Desmyter, A., Decanniere, K., Muyldermans, S., and Wyns, L. (2001). Antigen specificity and high affinity binding provided by one single loop of a camel single-domain antibody. J Biol Chem *276*, 26285-26290.

Desmyter, A., Transue, T.R., Ghahroudi, M.A., Thi, M.H., Poortmans, F., Hamers, R., Muyldermans, S., and Wyns, L. (1996). Crystal structure of a camel single-domain VH antibody fragment in complex with lysozyme. Nat Struct Biol *3*, 803-811.

Holm, L., and Sander, C. (1993). Protein structure comparison by alignment of distance matrices. J Mol Biol *233*, 123-138.

Lefranc, M.P. (2005). IMGT, the international ImMunoGeneTics information system: a standardized approach for immunogenetics and immunoinformatics. Immunome Res *1*, 3.

Yanez, M.E., Korotkov, K.V., Abendroth, J., and Hol, W.G. (2008). The crystal structure of a binary complex of two pseudopilins: EpsI and EpsJ from the type 2 secretion system of Vibrio vulnificus. J Mol Biol *375*, 471-486.